

Diffraction efficiency of strong volume holograms

John H. Hong and Pochi Yeh

Rockwell International Science Center, 1049 Camino dos Rios, A25A, Thousand Oaks, California 91360

Demetri Psaltis and David Brady

Department of Electrical Engineering, California Institute of Technology, 116-81, Pasadena, California 91125

Received September 22, 1989; accepted January 2, 1990

We investigate the diffraction efficiency of strong volume holograms in which the coupling parameter is several times that needed for maximum diffraction efficiency. We discuss the implications of our findings on photorefractive implementations of various neural network systems.

The study of volume gratings has led to useful applications in many areas of optics, including integrated optics, acousto-optics, and holography. In most situations the coupled-mode analysis of volume holograms established by Kogelnik¹ accurately describes the diffraction behavior of a thick hologram and predicts a diffraction efficiency that is a periodic function of the index perturbation amplitude–thickness product. The diffraction efficiency η from a volume index grating with the direction of the readout beam tuned for the Bragg condition is given by

$$\eta = \exp(-\alpha d / \cos \theta) \sin^2(\pi \Delta n d / \lambda \cos \theta), \quad (1)$$

where α is the absorption coefficient, d is the thickness of the hologram, Δn is the amplitude of the index perturbation, and θ is the angle of incidence of the readout beam with respect to the normal to the surface of the hologram (we assume an unslanted grating); θ and λ are assumed to be measured inside the medium. Typically the amplitude of $\Delta n d$ realized in most holographic materials is such that only the increasing part of the first period of η is observed. As the grating amplitude and/or the thickness of the grating is increased beyond this regime, further coupling between the two waves results in a reversal of the energy-transfer direction to yield a drop in the diffraction efficiency as predicted by Eq. (1).

We have been able to observe this effect in a photorefractive barium titanate (BaTiO_3) crystal. The use of photorefractive crystals for such a purpose is particularly appropriate since the dynamic nature of photorefractive allows us to record easily and accurately the temporal evolution of Δn , the index change. For example, by monitoring η during the holographic recording process, we are able to observe the functional dependence of η on $\Delta n d$ from $\Delta n d = 0$ to saturation. Although η cannot exceed unity, a large saturation value of $\Delta n d$ is desirable because it corresponds to a large dynamic range for hologram recording, which in turn implies that a large number of holograms may be recorded. By monitoring the time dependence of η , we are able to estimate the saturation value of $\Delta n d$ in our BaTiO_3 sample and calculate the storage capacity of the crystal for dense holographic interconnections.

Such interconnections are useful in parallel information-processing applications such as artificial neural networks.^{2,3}

In a photorefractive crystal the steady-state value of Δn is proportional to the modulation depth of the intensity interference pattern responsible for writing the hologram. Hence, by manipulating the intensities of the writing beams, one can monitor the functional relationship between Δn and the diffraction efficiency. For a fixed writing-beam modulation depth, the entire range of index perturbation amplitudes from zero to the maximum attainable value can be scanned by performing a transient experiment in which one of the two writing beams is abruptly turned on and then turned off after permitting the grating to saturate. One beam is left on to ensure a zero-grating initial condition and also to provide an erasure mechanism after the other beam is turned off. Since the diffraction efficiency is a periodic function of Δn , for a sufficiently large saturation value of Δn the diffracted intensity will oscillate as a function of time during both formation and decay of the grating. The theoretical predictions of the temporal behavior of the index grating amplitude and its associated diffraction efficiency are plotted in Figs. 1(a) and 1(b), respectively. We see that the larger the saturation value of Δn , the more oscillations are present in η . The plots are shown for two values of the strength parameter given by $\phi = \pi \Delta n d / \lambda \cos \theta$. The saturation value of Δn can be easily controlled by adjustment of the writing-beam intensities.

We have written holograms in single-crystal BaTiO_3 using an argon-ion laser ($\lambda = 514.5$ nm) with a read beam derived from a He–Ne laser ($\lambda = 633$ nm). The experimental apparatus, shown in Fig. 2, is described below. The writing beam was polarized in the ordinary direction with respect to the crystal in order to preclude beam-coupling effects so that a uniform grating could be written in the crystal. The width of the writing beam was approximately 1 mm, and the power levels that were used are indicated in Fig. 3. The readout beam (≈ 1 -mm width, power level ~ 95 μW) is a He–Ne beam at $\lambda = 633$ nm that is polarized in the extraordinary direction and aligned at the Bragg angle

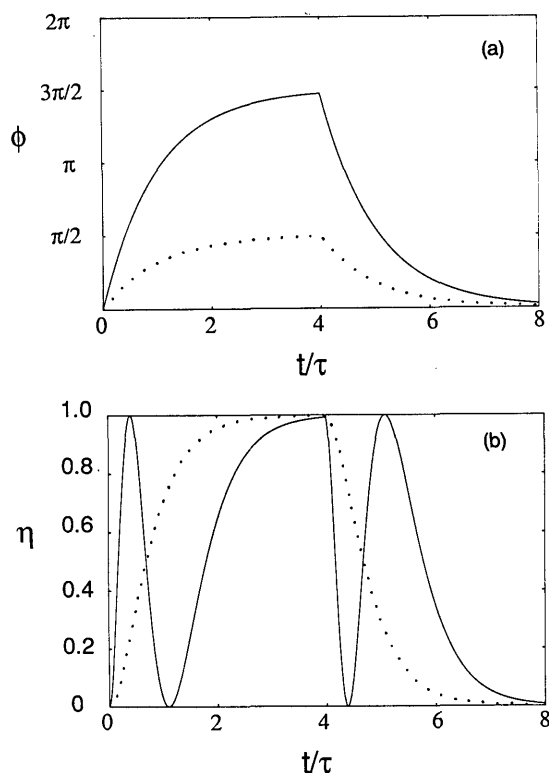


Fig. 1. Theoretical predictions of the temporal behavior of the strength parameter and diffraction efficiency during hologram development and erasure. Plots are given for two steady-state value of ϕ : $\phi_{\max} = \pi/2$ (dotted curve) and $\phi_{\max} = 3\pi/2$ (solid curve). The time is shown in units of the photorefractive time constant. (a) Growth and decay of the strength parameter ϕ . (b) Normalized diffraction efficiency during growth and decay of the grating [corresponding to depth parameter plots of (a)].

of the hologram. This combination of ordinary-extraordinary polarizations for the write-read beams gives maximum diffraction efficiency with minimum coupling. The relative intensities of the two writing beams can be adjusted with the variable attenuator realized by a wave plate-polarizing beam splitter combination. The 4-mm-thick BaTiO_3 crystal is a special-cut variety whose orientation was selected to access the large r_{42} coefficient [the c axis is oriented 30° from the cut face; see Fig. 2(b)].⁴ The special crystal cut effectively gives a large dynamic range for the index variation Δn that we can write.

The two writing beams were first turned on, and the readout-beam direction was adjusted for maximum diffraction efficiency. The intensity of one of the writing beams (#1) could be varied with a wave plate-polarizer combination. After shutting off beam #1 and waiting until the hologram was completely erased by the other beam, we abruptly turned beam #1 on again. After a steady state was achieved in the diffracted intensity, beam #1 was again shut off. The temporal evolution of the diffracted power exhibited oscillatory behavior, indicating that the Δn was varied through several peaks of the diffraction efficiency curve during the development and erasure of the hologram. The experiment was repeated for several dif-

ferent write-beam intensity ratios. The diffraction efficiency record for a near-unity beam intensity ratio exhibited the largest number (3) of oscillations [Fig. 3(c) corresponds to the near-unity beam intensity ratio hologram, and Fig. 3(a) corresponds to the smallest beam ratio hologram; note that the latter exhibits no oscillations during either formation or decay]. The oscillatory behavior compares favorably with the theoretical plots of Fig. 1, except that the experimental oscillations do not dip down to zero and the maxima have different values. This may be due to two-wave mixing between the reading beam and its diffracted component, the small but finite two-wave mixing between the two writing beams, and/or imperfections in the overlap between the hologram and the read beam. The maximum diffraction efficiency in each case was $\sim 25\%$, which differs from the ideal unity value owing to absorption, reflection losses, scattering, and position errors in setting the readout beam so that it maximally overlaps with the grating.

Volume holograms have long attracted interest for information-storage applications owing to their potentially large storage capacity and more recently as an interconnection device for neural networks. In such applications, holograms are superimposed within the same crystal volume where, for example, the reference beam can be angularly multiplexed to distinguish between the various holograms. The corresponding index perturbation of such a superposition can be expressed by

$$\Delta n(\mathbf{r}) \propto \sum_{m=1}^M f_m(\mathbf{r}), \quad (2)$$

where $f_m(\mathbf{r})$ is the contribution of the m th hologram and \mathbf{r} is the spatial coordinate within the volume. It is important to gauge the maximum number of holograms, M , that can be recorded in a given crystal. Although other constraints such as that due to geome-

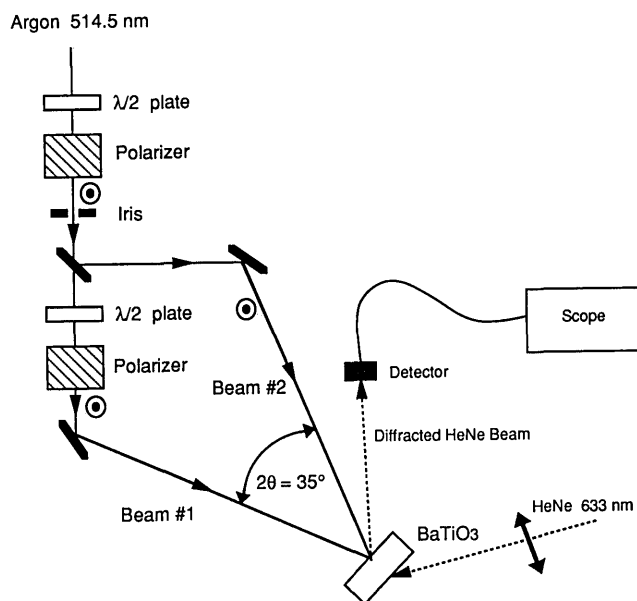


Fig. 2. Apparatus for writing and probing deep holograms.

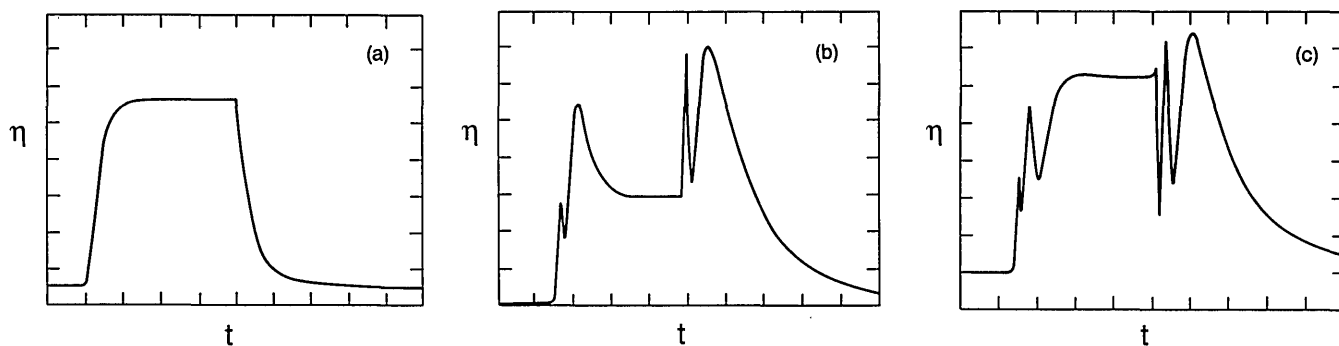


Fig. 3. Diffraction efficiencies recorded during writing and erasure of gratings. The peak diffraction efficiency in each case is approximately $25 \pm 3\%$ (diffraction efficiency is defined as the ratio of the input readout power to the diffracted power); the horizontal scale is 793.5 msec/division. (a) $P_1 = 24$ mW, $P_2 = 2.1$ mW; (b) $P_1 = 27.8$ mW, $P_2 = 10.8$ mW; (c) $P_1 = 20.7$ mW, $P_2 = 20.8$ mW.

try exist,^{2,3} we are interested in the limit on M as dictated by the finite dynamic range of photorefractive crystals. In particular, we use the maximum index modulation that we observed in our strong hologram experiments in conjunction with a reasonable figure for the smallest index modulation that can be detected to calculate the dynamic range that is available in BaTiO₃.

As is shown in Fig. 3(c), a hologram recorded at unity modulation depth in our BaTiO₃ sample achieved the third maximum of the diffraction efficiency function given in Eq. (1). This result implies a saturation strength parameter of $\phi_{\max} = 5\pi/2$ (for an approximate interaction length of $d = 4$ mm, which is the crystal thickness, this value of ϕ corresponds to $\Delta n = 1.67 \times 10^{-4}$). Given a minimum allowable diffraction efficiency per hologram of η_{\min} , the minimum allowable value for the strength parameter can be found in the small perturbation regime of Eq. (1) to be $\phi_{\min} \approx (\eta_{\min})^{1/2}$, where η_{\min} is determined from noise sources in the apparatus such as scattering and detector noise. Although the specific value of η_{\min} is dependent on the measurement environment (e.g., scattering and detector noise), the value of $\eta_{\min} = 0.01\%$ (1-mW/cm² read beam resulting in a 100-nW/cm² diffracted beam) is reasonable. The ratio of these two numbers gives the index amplitude dynamic range,

$$R = \frac{\phi_{\max}}{\phi_{\min}} = \frac{5\pi/2}{(\eta_{\min})^{1/2}} \approx 10^3. \quad (3)$$

Turning now to the multiple-hologram case, this dynamic range must be greater than or equal to the average amplitude excursions of the total superposition $\Delta n(\mathbf{r})$ given by relation (2) (normalized by the amplitude of each component of the sum) in order to maintain accuracy. In almost all cases of interest, the individual terms of the sum of relation (2) are mutually uncorrelated, so that the normalized amplitude excursion is $M^{1/2}$. Equating the dynamic range to $M^{1/2}$ yields $\phi_{\max} = \phi_{\min} M^{1/2}$, from which we get $M_{\max} = R^2 \approx$

10^6 , the maximum number of holograms that can be supported. Unfortunately, such a large number is difficult to realize in practice because of the additional constraint placed by incoherent erasure during the sequential exposure process used to achieve the superimposed set of holograms of relation (2). In particular, it is shown in Ref. 5 that the exposure schedule that must be followed in order to yield a set of holograms with equal amplitudes results in a strength parameter equal to ϕ_{\max}/M for each component. Under this constraint the maximum number of holograms is determined by the detectability of each component, so that

$$\frac{\phi_{\max}}{M} = \phi_{\min}, \quad (4)$$

which yields $M_{\max} = R \approx 10^3$. This value is consistent with the discussions and experiments found in Refs. 6 and 7.

This research is supported in part by the U.S. Office of Naval Research under contract N00014-88-C-0230. At the California Institute of Technology this research is supported by the Defense Advanced Research Projects Agency and the U.S. Air Force Office of Scientific Research.

References

1. H. Kogelnik, *Bell Syst. Tech. J.* **48**, 2909 (1969).
2. P. J. Van Heerden, *Appl. Opt.* **2**, 393 (1963).
3. H. Lee, X. Gu, and D. Psaltis, *J. Appl. Phys.* **65**, 2191 (1989).
4. Y. Fainman, E. Klancnik, and S. H. Lee, *Opt. Eng.* **25**, 228 (1986).
5. D. Psaltis, K. Wagner, and D. Brady, *Appl. Opt.* **27**, 1752 (1988).
6. W. J. Burke, D. L. Staebler, W. Phillips, and G. A. Alphonse, *Opt. Eng.* **17**, 308 (1978).
7. F. Mok, M. Tackitt, and H. M. Stoll, in *Digest of Annual Meeting of the Optical Society of America* (Optical Society of America, Washington, D.C., 1989), p. 76.